doi:10.1093/brain/awv002 BRAIN 2015: 138; 992–1008 | 992

BRAIN
A JOURNAL OF NEUROLOGY

# Neuronal death induced by misfolded prion protein is due to NAD$^+$ depletion and can be relieved *in vitro* and *in vivo* by NAD$^+$ replenishment

**Minghai Zhou,[1] Gregory Ottenberg,[1,*] Gian Franco Sferrazza,[1,#] Christopher Hubbs,[2] Mohammad Fallahi,[3] Gavin Rumbaugh,[2] Alicia F. Brantley[4] and Corinne I. Lasmézas[1]**

The mechanisms of neuronal death in protein misfolding neurodegenerative diseases such as Alzheimer's, Parkinson's and prion diseases are poorly understood. We used a highly toxic misfolded prion protein (TPrP) model to understand neurotoxicity induced by prion protein misfolding. We show that abnormal autophagy activation and neuronal demise is due to severe, neuron-specific, nicotinamide adenine dinucleotide (NAD$^+$) depletion. Toxic prion protein-exposed neuronal cells exhibit dramatic reductions of intracellular NAD$^+$ followed by decreased ATP production, and are completely rescued by treatment with NAD$^+$ or its precursor nicotinamide because of restoration of physiological NAD$^+$ levels. Toxic prion protein-induced NAD$^+$ depletion results from PARP1-independent excessive protein ADP-ribosylations. *In vivo*, toxic prion protein-induced degeneration of hippocampal neurons is prevented dose-dependently by intracerebral injection of NAD$^+$. Intranasal NAD$^+$ treatment of prion-infected sick mice significantly improves activity and delays motor impairment. Our study reveals NAD$^+$ starvation as a novel mechanism of autophagy activation and neurodegeneration induced by a misfolded amyloidogenic protein. We propose the development of NAD$^+$ replenishment strategies for neuroprotection in prion diseases and possibly other protein misfolding neurodegenerative diseases.

1 Department of Infectious Diseases, The Scripps Research Institute, Scripps Florida, Jupiter, FL 33458, USA
2 Department of Neuroscience, The Scripps Research Institute, Scripps Florida, Jupiter, FL 33458, USA
3 Informatics Core, The Scripps Research Institute, Scripps Florida, Jupiter, FL 33458, USA
4 Behaviour Core, The Scripps Research Institute, Scripps Florida, Jupiter, FL 33458, USA

*Current address: Department of Chemistry, The Scripps Research Institute, Scripps Florida, USA
#Current address: Apple Inc, Cupertino, CA 95014, USA

Correspondence to: Corinne Lasmézas, DVM, PhD,
The Scripps Research Institute,
Scripps Florida,
130 Scripps Way 2B2,
Jupiter,
FL 33458, USA
E-mail: lasmezas@scripps.edu

**Keywords:** protein misfolding; prion; neurodegeneration; nicotinamide dinucleotide; neuroprotection

**Abbreviations:** NAD = nicotinamide adenine dinucleotide; TPrP = toxic prion protein

Received June 19, 2014. Revised October 16, 2014. Accepted November 24, 2014. Advance Access publication February 12, 2015

# Introduction

Prion diseases are fatal brain diseases of animals and humans and belong to the group of protein misfolding neurodegenerative diseases such as Alzheimer's, Parkinson's, and Huntington's diseases, frontotemporal dementia or amyotrophic lateral sclerosis. The common feature of these diseases is that their aetiology is linked to the misfolding and aggregation of a host protein. For a long time, it was thought to be a peculiarity of prion diseases that highly aggregated forms of the prion protein PrP called $PrP^{Sc}$ (Prusiner, 1982), possibly associated with other molecules, are transmissible from cell to cell and from organism to organism, making prion diseases infectious. However, it is becoming increasingly clear that aggregated forms of other amyloidogenic proteins such as amyloid-β, α-synuclein, tau or SOD1 can also spread from cell to cell *in vitro* and *in vivo* (Aguzzi and Rajendran, 2009; Garden and La Spada, 2012; Olanow and Brundin, 2013), revealing a new common pathobiological feature of several protein misfolding neurodegenerative diseases, even though the distinction needs to be made between intercellular transmission and infectiousness.

Understanding the mechanisms by which these misfolded proteins trigger neurodegeneration remains a challenge. Apoptosis and autophagy induction/dysfunction occur in Alzheimer's disease, Parkinson's disease, Huntington's disease, amyotrophic lateral sclerosis and prion diseases (Liberski *et al.*, 1992; Nixon *et al.*, 2005; Martinez-Vicente and Cuervo, 2007; Martinez-Vicente *et al.*, 2010; Winslow and Rubinsztein, 2011; Zhou *et al.*, 2012). Autophagy is an important mechanism of clearance of misfolded proteins and damaged organelles (Martinez-Vicente and Cuervo, 2007; Heiseke *et al.*, 2009). However, both the role of apoptosis and the exact function of autophagy in the death cascade are still under investigation.

Establishing relevant cellular models to study neurotoxicity mechanisms is another challenge. Amyloid pathology does not always correlate with neuronal dysfunction and degeneration (Crystal *et al.*, 1988; Büeler *et al.*, 1994; Lasmézas *et al.*, 1997; Dorandeu *et al.*, 1998; Piccardo *et al.*, 2007; Sandberg *et al.*, 2011; Zetterberg and Blennow, 2013). In the meantime, it has become increasingly clear in the protein misfolding neurodegenerative disease field that neurotoxicity is due to soluble misfolded forms of the cognate amyloidogenic proteins (Caughey and Lansbury, 2003; Lesne *et al.*, 2006; Haass and Selkoe, 2007; Outeiro *et al.*, 2008; Winner *et al.*, 2011; Benilova *et al.*, 2012). Therefore, small oligomers of various sizes of the amyloid-$\beta_{42}$ peptide are used to study Alzheimer's disease (Benilova *et al.*, 2012). Overexpression of α-synuclein or toxin models is widely used in the field of Parkinson's disease (Blesa *et al.*, 2012). In addition, exogenous preparations of α-synuclein have been shown to induce cytotoxicity (Kayed *et al.*, 2003; Luk *et al.*, 2012; Braidy *et al.*, 2013). Because of the existence of familial forms of these diseases, overexpression of mutated proteins is also used to model Alzheimer's, Parkinson's, Huntington's or prion diseases (Ma *et al.*, 2002; Friedman-Levi *et al.*, 2011; Trancikova *et al.*, 2011).

In-depth study of neurodegenerative mechanisms in prion diseases has been hampered for many years by the lack of an experimental *in vitro* model. We identified a misfolded monomeric form of PrP (TPrP) as the most neurotoxic PrP entity, with activity *in vitro* and *in vivo* in the nanomolar range, neuronal specificity and reproduction of key molecular and pathological hallmarks of prion diseases such as apoptosis and the formation of autophagic vacuoles (Zhou *et al.*, 2012). The non-toxic monomeric PrP counterpart (non-toxic PrP) is used as control. The exquisite neuron-specific toxicity of TPrP reproduces a feature of prion diseases, namely that prion-induced pathology is restricted to the CNS despite prion replication in peripheral organs (Unterberger *et al.*, 2005). The TPrP toxicity model is highly reproducible, dosable and portable *in vitro* and *in vivo*; therefore, we used it to study neurodegenerative mechanisms.

In the present study, we show that apoptosis and autophagy are not primary players in the death cascade as their pharmacological modulation does not significantly modify neuronal demise of TPrP-exposed neurons. On the other hand, we discovered that TPrP induces neuronal death via a profound depletion of intracellular nicotinamide adenine dinucleotide ($NAD^+$) levels causing metabolic failure. Neuronal death can be rescued *in vitro* and *in vivo* by $NAD^+$ replenishment. Intranasal treatment of mice with $NAD^+$ during established prion disease significantly delayed motor impairment. $NAD^+$ donates its ADP-ribose moiety during the post-translational modifications ADP-ribosylations that transfer single or multiple ADP-ribose units onto proteins, and are performed by mono-ADP-ribosyltransferases (mARTs) or poly-ADP-ribosylpolymerases (PARPs) (Hottiger *et al.*, 2010), respectively. Thus ADP-ribosylations are $NAD^+$ consuming reactions. Although $NAD^+$ depletion induced by PARP1 has been implicated in other brain conditions such as excitotoxicity, oxidative stress and brain ischaemia (Zhang *et al.*, 1994; Eliasson *et al.*, 1997; Alano *et al.*, 2010; Kuzhandaivel *et al.*, 2010; Andrabi *et al.*, 2011), our data demonstrate for the first time that a failure of $NAD^+$ metabolism is the cause of neuronal ailing following exposure to a misfolded amyloidogenic protein, and is reversible. Moreover, our TPrP toxicity model reveals a new mechanism of $NAD^+$ depletion independent of PARP1.

# Materials and methods

## Production of recombinant prion proteins

TPrP and non-toxic PrP were produced as described (Zhou *et al.*, 2012). Briefly, full-length murine $PrP_{23–230}$ was purified

from inclusion bodies in *Escherichia coli* transfected with pET30a (Novagen) containing the murine $PrP_{23–230}$ cDNA. PrP was then solubilized in 8 M urea and recovered after dilution refolding. Refolded soluble PrP was then fractionated with a phosphate-buffered saline (PBS) running buffer (pH 7.4) using a Superdex$^{TM}$ 200 16/60 column (GE Healthcare Life Sciences), and the TPrP and non-toxic PrP fractions eluting at volumes V89 to V93 and V109, respectively, were collected. Toxicity of each batch of TPrP was confirmed by toxicity assay in PK1 cells. Protein concentration was measured using the bicinchoninic acid test (Pierce) and the preparations were stored at −80°C.

## Cell culture, treatments and microscopy

Murine PK1 cells (a subclone of murine N2a neuroblastoma cells kindly provided by C. Weissmann) were cultured in Opti-MEM® containing 5% bovine growth serum (Invitrogen). Cells were plated in 96-well plates for toxicity assays and 24-well plates or 96-well plates for $NAD^+$ measurements. Medium was supplemented with any of $Fe(NO_3)_3.9H_2O$ (Alfa Aesar), L-cystine.2HCl, L-glutamine, choline chloride, folic acid, D-pantothenic acid, thiamine.HCl, $NAD^+$, NADH (all Mp Biomedicals), ATP (Thermo Scientific), myo-inositol (Alexis Biochemicals), pyridoxine.HCl (Fisher Bioreagent), riboflavin (Acros Organics) Eagle's minimal essential medium, Dulbecco's modified Eagle medium (DMEM; ATCC), Z-VAD-FMK (BD Biosciences Pharmingen), rapamycin, 3-methyl adenine, bafilomycin A1 (Sigma), sucrose (Acros Organics), chloroquine (Mp Biomedicals Inc), L-ascorbic acid (Fisher Chemical), nicotinamide (Indofine chemical company), FK866 (Cayman chemical company), resveratrol, AGK2, 2,2'-dihydroxyazobenzene (DAB, Sigma), benzamide, 3-aminobenzamide (3-ABA, Sigma), 6-nitroso-1,2-benzopyrone (NBP, Sigma), *N*-(6-oxo-5,6-dihydro-phenanthridin-2-yl)-*N*,*N*-dimethylacetamide (PJ-34, Enzo Life Sciences), 2-[(2R)-2-Methylpyrrolidin-2-yl]-1*H*-benzimidazole-4-carboxamide dihydrochloride (ABT-888, veliparib, Enzo Life Sciences), 5-aminoisoquinolinone (5-AIQ, Enzo Life Sciences), TIQ-A and and 1,5-Isoquinoline diol (Enzo Life Sciences).

Primary cortical cultures were prepared as described (Rumbaugh *et al.*, 2006) with slight modifications. Neurons were harvested from newborn (postnatal Day 0) mice and dissociated neurons were maintained in Neurobasal® medium supplemented with B27 1x, GlutaMAX$^{TM}$ 2% and 2 µg/ml gentamycin. Neuronal cultures prepared with this method contain ~30% post-mitotic astroglia. Neurons were fed once on *in vitro* Day 4 and exposed to TPrP on *in vitro* Day 6. Astrocytes were obtained by treating the cultures with 10 nM FK866 for 3 days. Astrocytes were exposed to TPrP for 7 days and assayed for $NAD^+$ levels and viability.

Phase-contrast micrographs were taken with a Nikon inverted epifluorescence microscope.

## $NAD^+$ and ATP measurements

$NAD^+$ concentrations were measured using two different kits, both of them measuring total oxidized (NAD+) and reduced NAD (NADH). For both assays, manufacturer's instructions were followed to prepare the NADH standard and measure $NAD^+$/NADH concentrations. In Fig. 4, $NAD^+$ measurements were normalized by number of living cells. In Fig. 4A and B, 50 000 PK1 cells were seeded in 24-well microtitre plates and $NAD^+$ was measured using the $NAD^+$/NADH quantification kit (BioVision) with absorbance read at OD 450 nm. In Fig. 4C, $NAD^+$ and ATP measurements were performed in parallel in 96-well plates seeding 3000 cells per well. $NAD^+$ was measured using the NAD/NADH-Glo$^{TM}$ quantitation kit (Promega) with a luminescence read-out. In Fig. 5C, cellular $NAD^+$ levels were measured using NAD/NADH-Glo$^{TM}$. Both $NAD^+$/NADH quantification assays used are cycling assays measuring total amounts of the metabolite, and are equivalent. ATP levels were measured after counting the number of cells using the luminescent assay (CellTiter-Glo®, Promega) according to the manufacturer's instructions. All signals were quantified at 610 nm using a Fluoroskan Ascent FL (ThermoElectron Corporation) and standardized by cell number.

## Western blot detection of cellular ADP-ribosylated proteins and poly-ADP ribose polymers in TPrP-exposed neuroblastoma cells

PK1 cells were treated in 24-well plates with 5 µg/ml TPrP (controls: 5 µg/ml non-toxic PrP or untreated). Cells were treated by TPrP in the presence of 9 nM FK866 (to inhibit $NAD^+$ synthesis from nicotinamide present in the culture medium) and 35 µM biotin-$NAD^+$ (Trevigen) or 25 µM non-biotinylated $NAD^+$ control. Cells were harvested after 2 days of treatment. Cell lysates were analysed by SDS-PAGE, transferred onto a nitrocellulose membrane. Biotinylated proteins, indicative of the incorporation of biotinylated ADP-ribose from the biotin-$NAD^+$ precursor, were revealed using streptavidin-HRP. Poly-ADP ribose polymers were analysed by western blot in untreated, non-toxic PrP or TPrP-treated PK1 neurons using the monoclonal anti-PAR antibody 10H (Enzo Life Sciences).

## Cell viability assays

Cells were plated in 96-well microtitre plates (1000 to 3000 cells per well) and cultured in 200 µl medium. Cell viability was measured using the luminescent assay CellTiter-Glo® (Promega) in all instances except for Fig. 4D where both CellTiter-Glo® and the fluorescent assay alamarBlue® (Life Technologies) were used for the purpose of comparing the outcome of CellTiter-Glo® with that of another viability assay. Assays were used according to the manufacturer's instructions. Signals were quantified using a Fluoroskan Ascent FL (ThermoElectron Corporation). For CellTiter-Glo®, units are relative light units (RLU). For alamarBlue®, units represent fluorescence intensity.

## Animal experiments

All mouse experiments were approved by the Institutional Animal Care and Use Committee (IACUC) of The Scripps Research Institute (TSRI), Scripps Florida. TSRI, Scripps Florida maintains a centralized animal care and use program

registered by the USDA, assured with the Office of Laboratory Animal Welfare (OLAW) and accredited by the Association for Assessment and Accreditation of Laboratory Animal Care, International (AAALAC). Housing and care of animals is consistent with the Public Health Service (PHS) Policy on Humane Care and Use of Laboratory Animals, The Guide for the Care and Use of Laboratory Animals the Animal Welfare Act, and other applicable state and local regulations.

## *In vivo* TPrP toxicity and $NAD^+$ rescue

Mice were anaesthetized with isoflurane and 2 µl of non-toxic PrP (0.7 µg/µl) or TPrP (0.14 µg/µl) with or without 20 µM or 100 µM $NAD^+$ were injected above the hippocampus of 12-week-old female C57BL/6J mice at 0.4 µl/min (stereotaxic coordinates −1.7 mm bregma, ± 2.00 mm lateral, and 1.75 mm ventral) using a stereotaxic frame (Dual Digital Small Animal Stereotaxic Instrument, Model 942, David Kopf Instruments). PBS was injected in the contralateral hemisphere as control. Each TPrP preparation was injected into four mice. Mouse brains were examined histopathologically after Nissl staining, 5 days after the injection. Mice were euthanized by $CO_2$ followed by cervical dislocation.

## $NAD^+$ treatment of prion-infected mice

Eight-week old female C57BL/6 mice were inoculated intracerebrally with 20 µl of 1% RML scrapie-infected brain homogenate. Starting at either 117 days post-inoculation (dpi) (Experiment 1) or 130 dpi (Experiment 2), five mice were treated daily by intranasal administration of 40 µl $NAD^+$ at 30 mM corresponding to a dose of 30 mg/kg. Control mice ($n = 5$) received the same volume of PBS. For intranasal administration, mice were held back down and the solution was administered progressively by placing 1–2 µl drops between the nostrils repeatedly after inspiration of the previous drop. Mice were monitored for the occurrence of clinical signs (overall activity, rigidity of tail/hindlimbs, ataxic gait, reduced grooming, kyphosis, weight loss) and euthanized at terminal stage of prion disease. In Experiment 1, weight curves were established. In Experiment 2, based on the observations made in Experiment 1, we quantified activity in the open field, motor performance and duration of terminal motor impairment. Survival times are given as means ± SDs.

## Rotarod test

The rotarod test measures motor balance and coordination as well as motor learning if performed on successive days. Mice were placed on a rotating rod ~30 mm in diameter that has an adjustable speed setting. The speed of the rotating rod was gradually increased from 2 to 20 rpm over a 5-min period, and latency to fall from the rod was recorded. Performance was tested from 137 dpi until the day mice stayed on the rotating rod for <30 s. Mice underwent three trials each day, with 30 min intertrial interval. Daily averages were calculated for each mouse, and group averages ± standard error of the mean (SEM) were calculated for each day.

## Open field

To assess general activity, locomotion and anxiety, mice were videotaped while allowed to freely move in Plexiglas® cages. To avoid biases, mice from the control and $NAD^+$ groups were videotaped simultaneously, and none of the mice had been manipulated prior to the recording. Scoring of movements was performed by author A.F.B. blinded to the treatment groups. The activity of the mice captured in the video (Supplementary material) was quantified by counting the number of line crossings during the entire recording time (2 min).

## Statistical analyses

Statistical analyses were performed using Prism v5 software. Unpaired two-tailed *t*-test was used to assess the delay in motor impairment of $NAD^+$-treated mice and the activity in the open field. One-way ANOVA followed by Dunnett's multiple comparison test was used for data shown in Figs 1A, 2A and B, 4B and C, 5A and B, and Supplementary Figs 1, 2, 4 and 5B. One-way ANOVA followed by Tukey's multiple comparison test was used for data shown in Figs 2C, 3, 4A, 5C, 6, and Supplementary Figs 3 and 6. For all figures, statistically significant differences (when compared to the controls mentioned in the legends) are shown using the following key: $^*P < 0.05$; $^{**}P < 0.01$; $^{***}P < 0.001$.

# Results

## Apoptosis and autophagy alterations are not the primary causes of cell death in TPrP-exposed neuroblastoma cells

We previously demonstrated that TPrP induces caspase 8- and 9-dependent apoptosis in neuroblastoma cells, as well as abnormal activation of the autophagic pathway as evidenced by an increased LC3II/I protein ratio and elevated lysosomal marker LAMP2 (Zhou *et al.*, 2012). We therefore first investigated if apoptosis or autophagy were the cause of neuronal death. The pan-apoptosis inhibitor Z-VAD had no effect on survival of TPrP-treated cells (Supplementary Fig. 1A). Neither induction of autophagy using the mTOR inhibitor rapamycin, nor blocking the early or late stages of autophagy using 3-MA and bafilomycin A1, respectively, significantly improved the survival of TPrP-treated cells (Supplementary Fig. 1B–D). We reasoned that toxicity may result from insufficient lysosomal capacity to process an excess of incoming autophagosomes induced by TPrP. We therefore used sucrose to increase lysosomal biogenesis. However, this did not improve neuronal survival (Supplementary Fig. 1E). To test the reverse hypothesis, namely that excessive lysosomal digestion would exert a cytotoxic effect, we blocked lysosomal function using chloroquine. Again, the latter had no effect on TPrP-induced cell death (Supplementary Fig. 1F). Finally,

treatment with the potent antioxidant ascorbic acid to protect TPrP-exposed cells against oxidative stress did not improve cell survival either (Supplementary Fig. 1G).

## Nicotinamide and NAD$^+$ rescue TPrP-injured neuroblastoma cells

We observed that the addition of culture medium 2 days after TPrP exposure delayed neuroblastoma cell death in a dose-dependent manner even in the continued presence of TPrP. The addition of PBS was not protective, ruling out a simple dilution effect. The protective effect conferred by DMEM was more potent than that of other culture media from which we inferred that the relevant component was present at higher concentration in DMEM than in other culture media (Supplementary Fig. 2A). We therefore tested every medium component that was present at higher concentration in DMEM than in other media (shown in Supplementary Fig. 2B). Only nicotinamide conferred protection against TPrP-induced cell death (Supplementary Fig. 2B) and it did so in a dose-dependent manner (Fig. 1A). Addition of nicotinamide 3 days after TPrP exposure clearly showed its capacity to reverse the pathological phenotype presented by TPrP-injured cells (rounded cells, abundant vacuolation). Neuritic regrowth and resorption of vacuoles occurred as soon as 3 h after addition of nicotinamide (Fig. 1B).

In mammalian cells, NAD$^+$ is mainly synthesized through the salvage pathway using the precursor nicotinamide. The *de novo* biosynthetic pathway, starting from the amino acid tryptophan, is not sufficient to sustain physiological NAD$^+$ concentrations in mammalian cells (Di Girolamo *et al.*, 2013). Because of this crucial role of nicotinamide in NAD$^+$ metabolism, we tested the protective effect of NAD$^+$. Addition of NAD$^+$ 3 days after TPrP exposure completely and dose-dependently rescued cells from TPrP-induced death (Fig. 2A). The rescuing effect of NAD$^+$ was independent of the reduced or oxidized status of the metabolite (Fig. 2B). Blockage of the salvage synthesis pathway (that uses nicotinamide as a precursor for NAD$^+$) using the compound FK866 abolished the protective effect of nicotinamide in a dose-dependent manner (but not that of NAD$^+$ itself), demonstrating that the effect of nicotinamide was indeed due to its role as a precursor of NAD$^+$ (Fig. 2C).

The protective effect of NAD$^+$ was specific for TPrP toxicity, since NAD$^+$ did not protect neuroblastoma cells against toxicity induced by autophagy modulators or the translation inhibitor cycloheximide (Supplementary Fig. 3).

## NAD$^+$ protects primary neurons against TPrP

We verified the protective effect of NAD$^+$ replenishment in primary cortical neurons. Of note, in our cultures ~30% of the culture plate surface is covered by post-mitotic astroglia. Neurobasal® culture medium used to obtain high quality primary neurons contains high levels of protective nicotinamide, preventing observation of TPrP toxicity. Therefore, we blocked NAD$^+$ synthesis from nicotinamide by addition of the inhibitor of the salvage pathway FK866 and added 20 or 40 μM NAD$^+$ to restore neuronal viability close to that of control cells (Supplementary Fig. 4). TPrP was toxic to primary neuronal cell cultures (Fig. 3A, compare lanes 3 and 9; lanes 4 and 10) and addition of NAD$^+$ restored viability (Fig. 3A lanes 9 to 11 and Fig. 3B).

## TPrP induces neuron-specific NAD$^+$ starvation and energy failure

We reasoned that the protective effect of nicotinamide and NAD$^+$ might be due to NAD$^+$ deficiency in TPrP-treated cells and measured intracellular NAD$^+$ levels. The term NAD$^+$ refers to the metabolite independent of its redox status as the measurements were done by an enzymatic cycling assay including both the oxidized and the reduced forms. NAD$^+$ levels decreased ~10 times after 3 days of TPrP exposure and were normalized by nicotinamide treatment, confirming that the rescuing effect of nicotinamide was due to NAD$^+$ repletion. NAD$^+$ levels were not reduced in PK1 cells similarly treated with the control non-toxic PrP monomer (non-toxic PrP, Fig. 4A and B). NAD$^+$ being a critical co-enzyme for cellular energy metabolism, we measured both NAD$^+$ and ATP cellular contents as a function of time in TPrP-exposed PK1 cells (Fig. 4C). NAD$^+$ and ATP levels were quantified in PK1 cell lysates after normalizing by living cell number to provide intracellular concentrations of the metabolites. NAD$^+$ level was reduced by more than half after 24 h of TPrP exposure and > 10 times after 3 days. A progressive decrease of ATP levels followed that of NAD$^+$, albeit to a smaller extent.

NAD$^+$ is an essential cellular metabolite involved in energy production, redox homeostasis, $Ca^{2+}$ signalling and post-translational modifications. Therefore, the primary cause of cell death is likely due to the dramatic NAD$^+$ starvation *per se* inducing global metabolic failure.

The CellTiter-Glo® viability assay used to perform these studies is a widely used and sensitive assay for the measure of cell viability quantifying ATP production in a well. As we found that TPrP reduces intracellular ATP, we wanted to compare the read-out of TPrP toxicity provided by CellTiter-Glo® with that of a non ATP-based assay. We therefore compared cell viability in TPrP-exposed cells in a time-course experiment using CellTiter-Glo® and the alamarBlue® assay that uses cells' reducing power to measure the number of living cells. Both assays gave remarkably comparable overall results (Fig. 4D). Interestingly, CellTiterGlo® provided a lower estimate of cell viability at Days 3 and 4 due to the reduction of ATP production in remaining living cells.

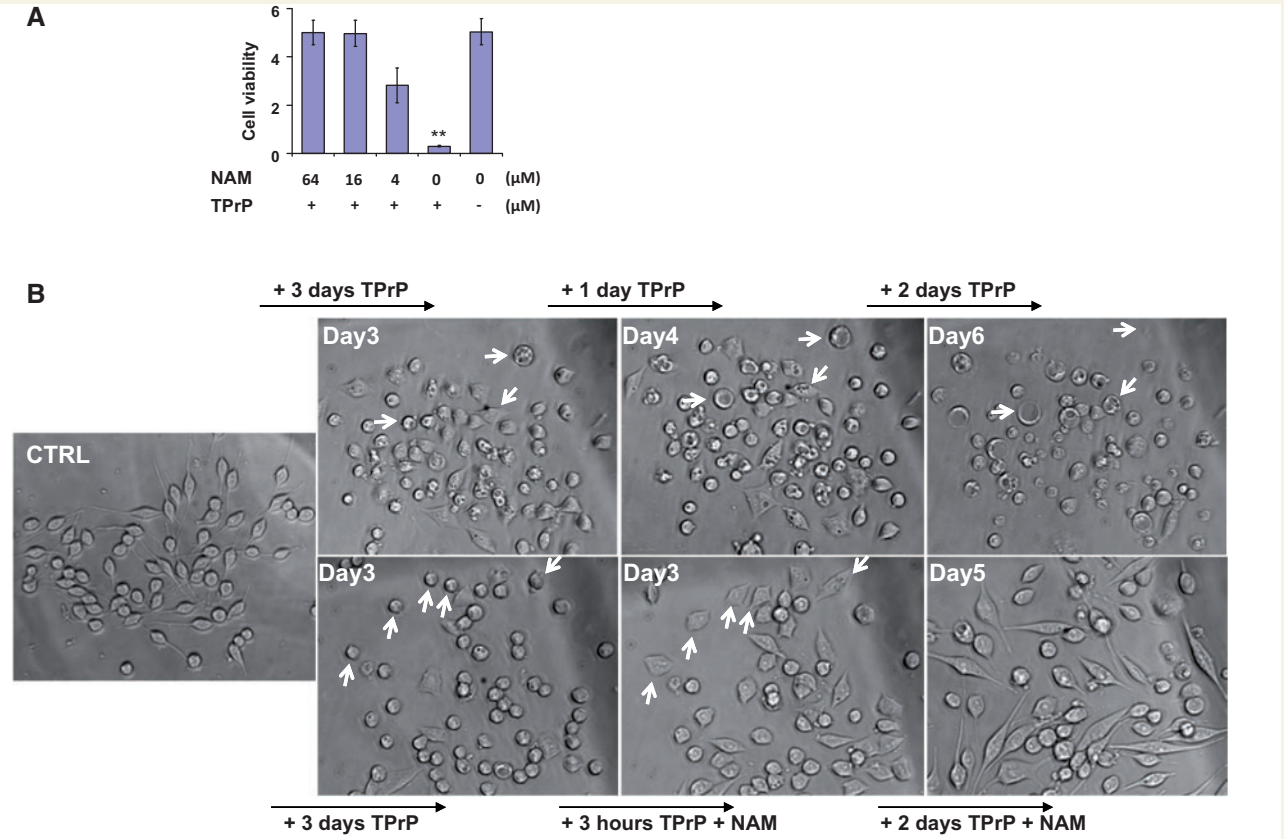


**Figure 1 Nicotinamide rescues TPrP-damaged neuroblastoma cells.** (**A**) Dose-dependent protection of nicotinamide against TPrP-induced toxicity (2.5 μg/ml TPrP). Nicotinamide was added at Day 3, cell survival measured at Day 5. Statistical differences are shown compared to the untreated control (**$P < 0.01$). Triplicate samples are shown with standard deviations. (**B**) Time-course phase-contrast micrographs illustrating the rescue of TPrP-injured neurons by nicotinamide. Nicotinamide (8 μg/ml) was added to neurons previously exposed to 5 μg/ml TPrP for 3 days (lower panels). At Day 3 post-TPrP exposure, neurons are rounded and vacuolated. In the absence of nicotinamide rescue (upper panels), at Day 4 vacuolation is severe, and at Day 6 most neurons are dead. Three hours after onset of nicotinamide treatment (lower panels), neurons resume their elongated shape and vacuoles disappear. Two days later, they harbour a perfectly healthy morphology. Pictures of cells exposed to TPrP in the presence or absence of nicotinamide treatment were taken from the same area in the cell culture to allow for a longitudinal study of the cell's fate. Arrows show examples of individual cell tracking. Individual cell follow-up was not possible at Day 2 post-nicotinamide treatment as healthy cells moved in the culture. The experiment was done four times.

We showed previously that TPrP exhibits neuron-specific toxicity (Zhou *et al.*, 2012), suggesting that TPrP triggers a neuron-specific death pathway. Supporting this hypothesis, primary astrocytes were not susceptible to TPrP toxicity and did not present $NAD^+$ depletion (Supplementary Fig. 6). In fact, $NAD^+$ levels were increased in TPrP-exposed astrocytes. We did not observe a decrease of $NAD^+$ levels in brain homogenates from mice at terminal stage of scrapie (data not shown). Prion pathology is characterized by extensive astrogliosis, with dying neurons being replaced by reactive astrocytes (Lasmézas *et al.*, 1996; Liberski and Brown, 2004). Therefore, we speculate that the absence of $NAD^+$ reduction in brains of scrapie mice is linked to this astrocytic reaction.

In summary, TPrP induces neuron-specific $NAD^+$ starvation, ATP deficiency and cell death, which can be prevented by $NAD^+$ replenishment. Next, we investigated the mechanism by which TPrP depletes $NAD^+$.

## TPrP induces excess ADP-ribosylation independent of PARP1

The redox cycle of $NAD^+$/NADH does not affect the overall cellular level of the metabolite. In contrast, there are several '$NAD^+$-consuming' cellular reactions performed by cellular enzymes that utilize $NAD^+$ as a co-factor: (i) the production of second messenger cyclic ADP-ribose (cADPR) and nicotinic acid adenine dinucleotide phosphate (NAADP) from $NAD^+$ by ADP-ribosyl cyclases (CD38 and CD157); (ii) protein deacetylations by sirtuins; and (iii) protein ADP-ribosylations by PARPs and mARTs (in which the ADP-ribose moiety of $NAD^+$ is transferred to proteins) (Houtkooper *et al.*, 2010). The first two possibilities seemed unlikely because an inhibitor of ADP-ribosyl cyclase (2,2'-dihydroxyazobenzene, DAB) and a sirtuin inhibitor (AGK2), did not modulate TPrP toxicity (Fig. 5A and B). Moreover, sirtuins act as 'sensors' for cellular

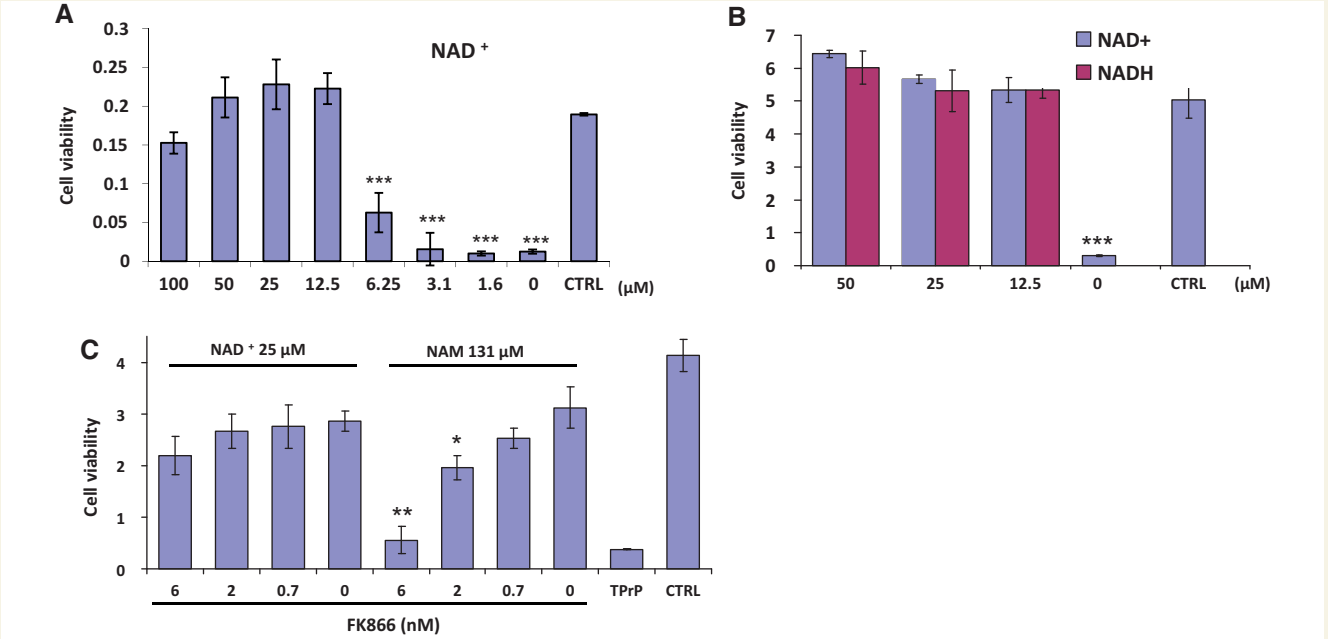


**Figure 2 NAD$^+$ rescues TPrP-damaged neuroblastoma cells.** (**A**) Dose-response of NAD$^+$ rescue of neuroblastoma cells from TPrP toxicity. Statistical differences are shown compared to untreated control (CTRL). The experiment was done three times in octaplicate wells; standard deviations are shown. (**B**) Both the oxidized (NAD$^+$) and the reduced (NADH) forms of the metabolite rescue neuroblastoma cells from TPrP death. Statistical differences are shown compared to CTRL. The experiment was done three times in triplicate wells; standard deviations are shown. (**C**) FK866, an inhibitor of the enzyme nicotinamide phosphoribosyltransferase (NAMPT) that regulates the rate-limiting step of the nicotinamide to NAD$^+$ synthesis pathway, abolishes nicotinamide, but not NAD$^+$ rescue, in a dose-dependent manner. Statistical differences in NAD$^+$ or nicotinamide-treated samples are shown compared to 0 NAD$^+$ or 0 nicotinamide, respectively, in the presence of FK866. The experiment was done twice in triplicate wells; standard deviations are shown. Cells were exposed to 2.5 μg/ml TPrP (**A** and **C**) or 5 μg/ml TPrP (**B**) for 5 days. NAD$^+$ or NADH was added at the indicated doses on Day 3 until Day 6, when cell viability was assessed. *$P < 0.05$; **$P < 0.01$; ***$P < 0.001$.

NAD$^+$ levels, i.e. adjust their activity to the level of available NAD$^+$ thereby being less likely to 'over-consume' NAD$^+$. On the other hand, high doses of the PARP1 inhibitor 3-ABA reproducibly mitigated TPrP-induced toxicity and replenished cellular NAD$^+$ (Fig. 5B and C). However, seven other PARP1 inhibitors [benzamide, 6-nitroso-1,2-benzopyrone (NBP), *N*-(6-oxo-5,6-dihydro-phenanthridin-2-yl)-*N*,*N*-dimethylacetamide (PJ-34), 2-[(2R)-2-Methylpyrrolidin-2-yl]-1*H*-benzimidazole-4-carboxamidedihydrochloride (ABT-888, veliparib), 5-aminoisoquinolinone (5-AIQ), TIQ-A and 1,5-Isoquinoline diol] were not effective, showing that the effect observed with 3-ABA was not due to its activity on PARP1 (Fig. 5B and C, and not shown, controls for the inhibitors' activity are shown in Supplementary Fig. 5). Others described that 3-ABA also inhibits mART activity (Yau *et al.*, 1998), thus we interpret the rescuing effect of this compound as due to its interference with mono-ADP-ribosylation.

To confirm this hypothesis, we directly assessed the extent of cellular protein ADP-ribosylation in TPrP-treated PK1 cells compared with non-treated cells or cells treated with non-toxic PrP. To this end, we treated cells with biotinylated NAD$^+$, leading to the incorporation of a biotin-labelled ADP-ribose moiety unto ADP-ribosylated proteins. Western-blot analysis of the latter using streptavidin-HRP revealed excessive protein ADP-ribosylation in TPrP-exposed cells (Fig. 5D, arrows). Moreover, TPrP did not lead to an increase of the PARP products poly-ADP ribose polymers (PARs, added on PARylated proteins) that are a hallmark of activation of PARP1 or other PARPs. PAR levels remained constant at first, then decreased at Day 1, correlating with the onset of NAD$^+$ deficiency (Fig. 5E). These data demonstrate that TPrP induces protein mono-ADP-ribosylation.

## NAD$^+$ protects hippocampal neurons from TPrP toxicity *in vivo*

Our results thus far suggested that NAD$^+$ deprivation is directly responsible for TPrP-induced neuronal death and that NAD$^+$ replenishment is key to protect against TPrP toxicity. We therefore assessed if the protective effect of NAD$^+$ holds true *in vivo*. To this end, we injected TPrP stereotaxically above the hippocampus of C57BL/6 mice. Similar to our previous description (Zhou *et al.*, 2012), TPrP, but not non-toxic PrP, induced extensive damage of the pyramidal neurons of the hippocampus. TPrP

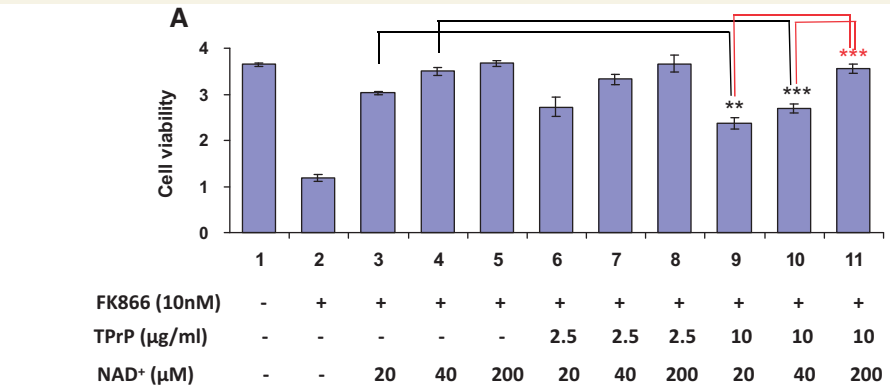


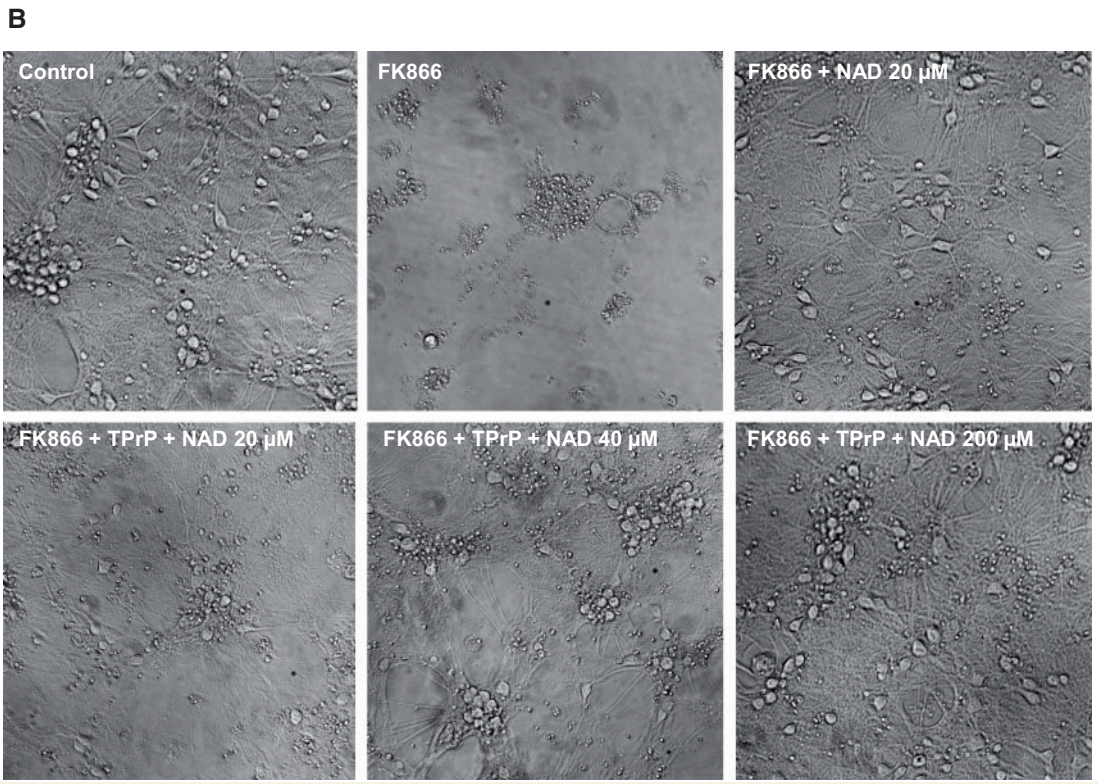


**Figure 3 NAD$^+$ protects primary neurons from TPrP-induced degeneration.** (**A**) Primary cortical neurons were treated at 6 days *in vitro* with FK866 and TPrP as indicated, and rescued with NAD$^+$. Cell viability was measured after 6 days of treatment. Statistical differences are shown compared to the matched controls as indicated in the graph. The experiment was done twice in duplicate wells; standard deviations are shown. (**B**) Where indicated, primary neurons were treated with 10 nM FK866, TPrP 10 µg/ml and NAD$^+$ (various doses) for 6 days. Phase contrast microscopy pictures were taken at Day 6 except for FK866 alone where the picture was taken at Day 5. Pictures are representative of two replicates. $^{**}P < 0.01$; $^{***}P < 0.001$.

toxicity could be abolished in a dose-dependent fashion by co-injection of NAD$^+$ (Fig. 6).

## NAD$^+$ treatment during the clinical phase of prion infection delays motor impairment

We then aimed at verifying the neuroprotective effect of NAD$^+$ against the toxicity of misfolded prion protein as produced in actual prion disease. Our *in vitro* studies showing rescue of TPrP-injured neurons even after the occurrence of overt signs of neuronal suffering (neuritic loss, extensive vacuolation) suggested that neuroprotection could be achieved therapeutically. We therefore performed two separate experiments to assess if NAD$^+$ treatment started at the onset or during the clinical phase of prion disease had a neuroprotective effect. Mice were treated daily with 30 mg/kg NAD$^+$ by the intranasal route as a means to

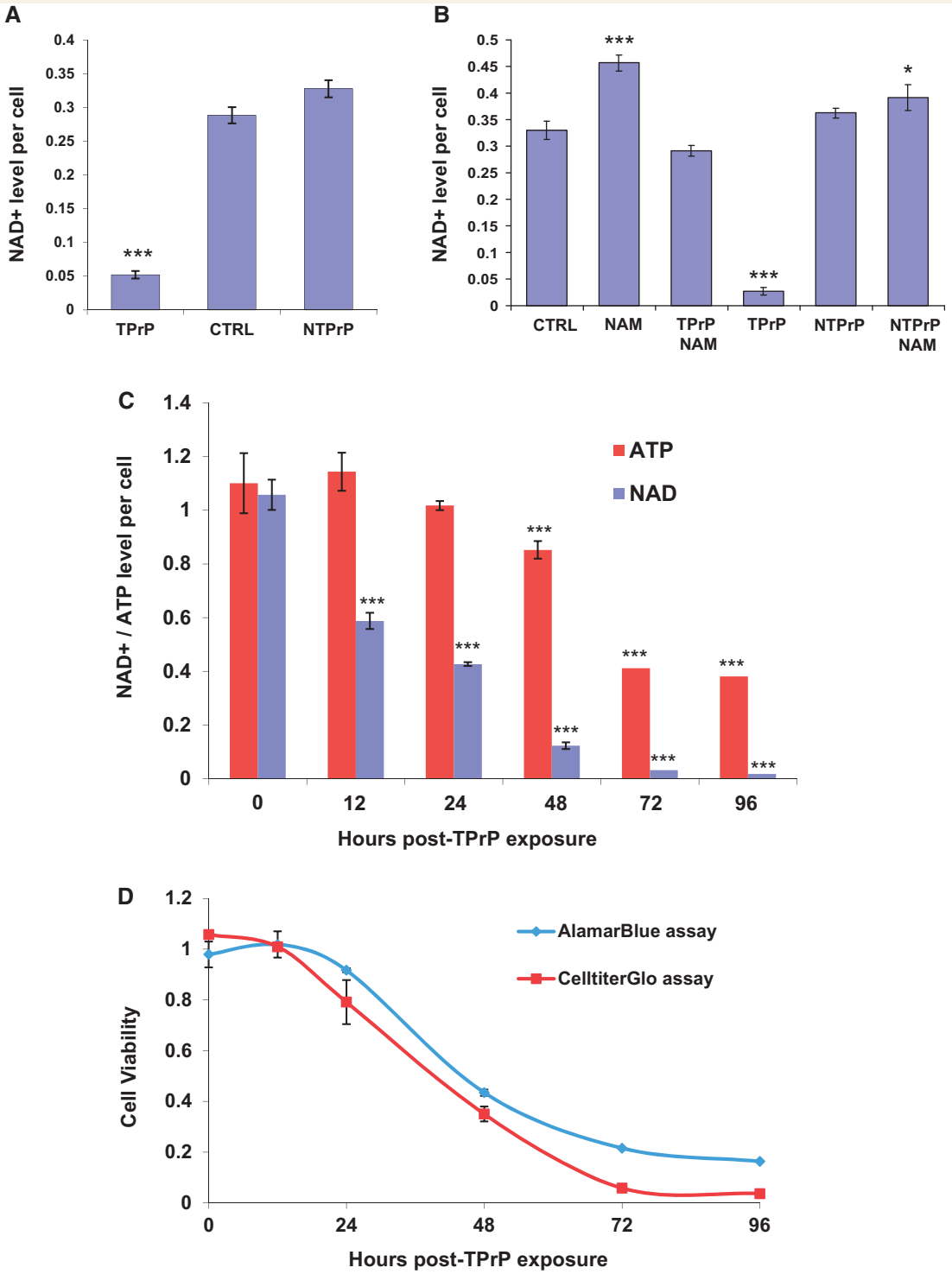


**Figure 4 TPrP induces depletion of intracellular NAD$^+$ and ATP.** (**A**) TPrP at 5 μg/ml for 3 days induces intracellular NAD$^+$ depletion, but not non-toxic PrP at 10 μg/ml. CTRL = untreated cells. Statistical differences are shown compared to CTRL. The experiment was done more than four times with duplicate samples; standard deviations are shown. (**B**) TPrP-induced NAD$^+$ depletion is corrected by the addition of nicotinamide (100 μg/ml). Cells were treated for 3 days with TPrP at 5 μg/ml or non-toxic PrP at 5 μg/ml. Statistical differences are shown compared to CTRL. The experiment was done twice with duplicate samples; standard deviations are shown. (**C**) TPrP induces a time-dependent decrease of intracellular NAD$^+$ (up to 200-fold) starting 12 h after TPrP exposure, correlating with a decrease of intracellular ATP (up to ~3-fold) starting 36 h later. Statistical differences are shown compared to the zero time point. The experiment was done three times in triplicate wells; standard deviations are shown. (**D**) Time course of TPrP-induced toxicity measured by CellTiterGlo® and AlamarBlue® assays. (**C** and **D**) TPrP was used at a dose of 5 μg/ml. The experiment was done twice with triplicate samples; standard deviations are shown. *$P < 0.05$; ***$P < 0.001$.

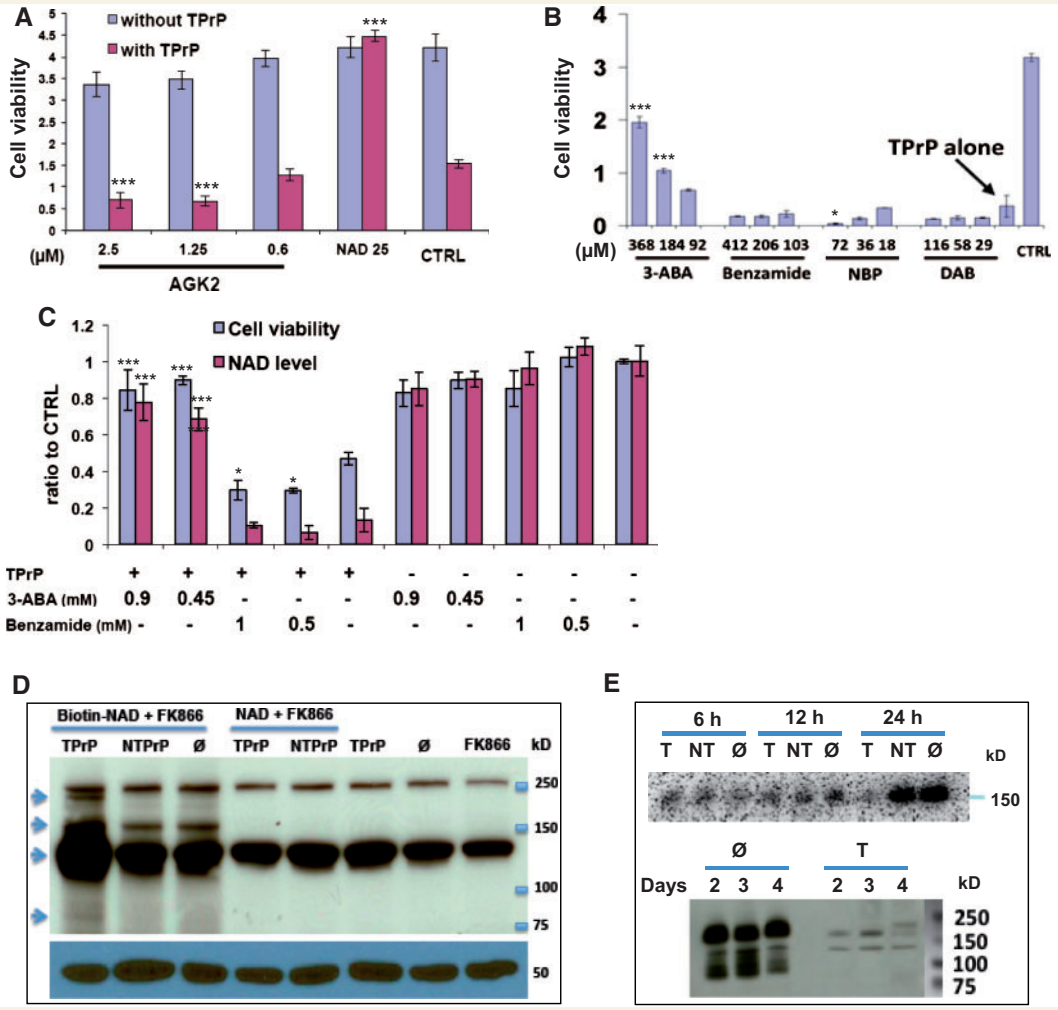


**Figure 5 TPrP induces over-ADP-ribosylation of proteins independent of PARP1.** (**A**) The sirtuin inhibitor AGK2 does not prevent TPrP toxicity. Cells were exposed to TPrP at 3.5 μg/ml and the compound for 4 days. NAD + (25 μM) was used as a rescue control. Statistical differences are shown for the TPrP-treated samples and are compared to the control (CTRL). The experiment was done in triplicate wells; standard deviations are shown. (**B**) Inhibition of ADP-ribosylation by 3-aminobenzamide (3-ABA) has a protective effect, but PARP1 inhibitors benzamide, 6-nitroso-1,2-benzopyrone (NBP) or the ADP-ribosyl cyclase inhibitor 2,2'-dihydroxyazobenzene (DAB) have no protective effect. Cells were exposed to TPrP at 2.5 μg/ml for 4 days, compounds were added after 2 days. Statistical differences are shown compared to TPrP treatment alone. The experiment was done twice in duplicate wells; standard deviations are shown. (**C**) Rescue from TPrP toxicity by 3-ABA is linked to $NAD^+$ restoration. Benzamide has no effect on cellular rescue or on intracellular $NAD^+$ levels. Cells were exposed to TPrP at 3.5 μg/ml and the compounds for 4 days. Statistical differences are shown for the TPrP-treated samples and are compared to TPrP treatment alone. The experiment was done in quadruplicate wells; standard deviations are shown. (**A–C**) Controls for the activity of the inhibitors are shown in Supplementary Fig. 5. (**D**) TPrP induces protein over-ADP-ribosylation. PK1 cells were supplied with biotin-$NAD^+$ and treated with FK866 (including a 6-h pretreatment) to prevent endogenous production of $NAD^+$ by the salvage synthesis pathway. The biotin-tag was incorporated into ADP-ribosylated proteins visualized using streptavidin-HRP. Cells exposed to TPrP for 2 days presented two additional ADP-ribosylated bands (arrows at ~220 kD and 80 kD) as well as bands of increased intensity (arrows at ~130 and 170 kD). Controls include non-toxic PrP treatment or absence of any form of PrP (ø); exogenous non-biotinylated $NAD^+$ was used as control for biotin-$NAD^+$. Additional controls were untreated cells or cells treated with FK866 alone. The two bands appearing on all lanes correspond to background signal. The bottom gel shows the tubulin loading control. The experiment was performed three times. (**E**) TPrP induces a reduction of poly-ADP ribose polymers (PARs), the products of PARP1. PARs were detected in PK1 neurons using the monoclonal anti-PAR antibody 10H after 6, 12, and 24 h of exposure to TPrP (T), non-toxic PrP (NT) or no protein (ø), or after 2, 3, and 4 days. A few faint additional bands visible at Day 4 in TPrP-treated cells likely represent PARylated proteins linked to secondary PARP1 activation as a consequence of apoptosis (observed after 3 days of TPrP treatment) and DNA-fragmentation. Samples (corresponding to biological duplicates) were normalized by protein amounts. The experiment was repeated for Days 1 and 2. *$P < 0.05$; ***$P < 0.001$.

circumvent the blood–brain barrier (Ross *et al.*, 2004; Graff and Pollack, 2005).

In the first experiment, mice were treated 117 days post-inoculation with RML prions and monitored for overall activity, clinical signs and weight loss. $NAD^+$-treated mice showed a slower disease progression and weight loss than mice from the PBS-treated control group, as shown in Fig. 7 and Supplementary Fig. 7. The extension of survival time

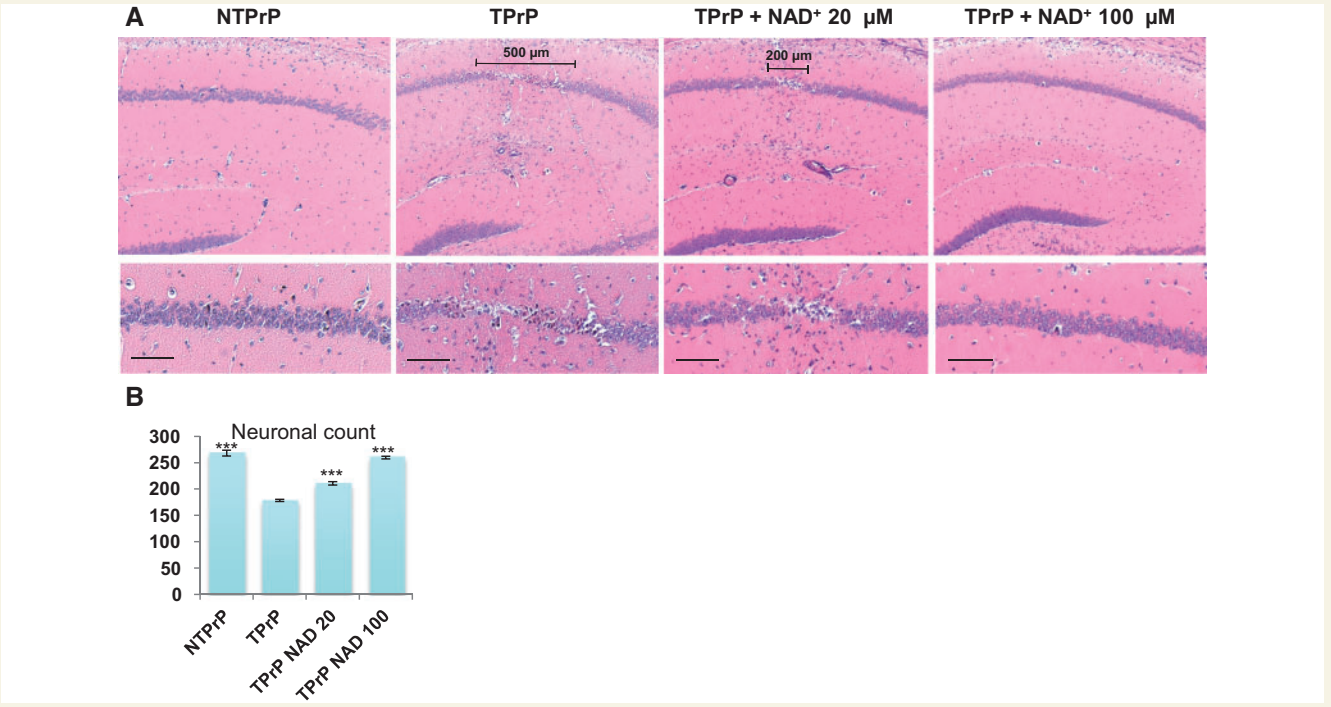


**Figure 6 NAD$^+$ protects hippocampal neurons from TPrP toxicity *in vivo*.** Non-toxic PrP (1.4 µg) or TPrP (0.28 µg) were injected stereotaxically in the presence or absence of NAD$^+$ and brains were examined after 5 days. Experiments were performed in quadruplicate. (**A**) The scale bars in the low magnification panels show the width of the damaged area. Upper panel: × 5 magnification; bottom panels: × 10 magnification (Scale bar = 100 µm). (**B**) Quantification was done on six brain sections taken at 20 µm intervals centred around the zone of maximal hippocampal damage. The number of pyramidal neurons in a 1000 µm linear area comprising $CA_2$ was counted using the MetaMorph™ software. Statistical differences are shown compared to brains injected with TPrP alone. Values shown are means ± SD. ***$P < 0.001$.

(PBS, 146 ± 8 days; NAD$^+$, 154 ± 2 days) was not statistically significant. Nonetheless, we visually observed a substantial improvement in overall activity and motor skills in the NAD$^+$-treated group. We thus decided to quantify these parameters in a subsequent experiment.

In the second experiment, daily NAD$^+$ treatment started at 130 days post-inoculation when RML-infected mice presented symptoms of prion disease such as a hunched posture and hindlimb rigidity when walking. We monitored overall activity and locomotion in an open field setting. Four days after the onset of treatment, we observed a substantial difference in the level of activity of NAD$^+$- versus PBS-treated mice. The former started moving and exploring almost immediately after being placed in the cage, while the majority of the latter remained prostrated (Supplementary Video 1). Rotarod testing starting 1 week after the onset of treatment showed better performance in NAD$^+$- versus PBS-treated mice (Supplementary Fig. 8). Quantification of motor activity in the open field showed a significant difference between the two groups (Fig. 7C). Although we did not observe a difference in survival times between the two groups (PBS, 159 ± 8 days; NAD$^+$, 160 ± 5 days), NAD$^+$ treatment significantly reduced the period of time during which mice suffered from severe motor impairment, showing protection of their motor function (Fig. 7D).

# Discussion

Pathobiological mechanisms prevailing in protein misfolding neurodegenerative diseases include mitochondrial dysfunction leading to increased reactive oxygen species, oxidative stress, reduced energy production, alteration of calcium homeostasis, cytochrome *c* release and activation of the intrinsic apoptotic pathway (Alzheimer's disease, Huntington's disease, Parkinson's disease) (Cavallucci *et al.*, 2012; Exner *et al.*, 2012; Zheng and Diamond, 2012). Other toxic mechanisms involve excitotoxicity via glutamate receptors (Alzheimer's disease, Parkinson's disease, prion diseases), oxidative stress, endoplasmic reticulum stress, translational repression and blockage of the ubiquitin-proteasome system (Huntington's disease, prion diseases) (Kristiansen *et al.*, 2007; Soto and Satani, 2011; Cavallucci *et al.*, 2012; Moreno *et al.*, 2012; Zheng and Diamond, 2012; Biasini *et al.*, 2013; Sonati *et al.*, 2013; Thellung *et al.*, 2013). Prominent alterations of the autophagolysosomal pathway are observed in all these diseases, encompassing deficient mitophagy (Parkinson's disease), cargo uptake (Huntington's disease), chaperone-mediated autophagy (Parkinson's disease), or autophagosomal clearance (Alzheimer's disease, Parkinson's disease, prion diseases, amyotrophic lateral sclerosis) (Heiseke *et al.*, 2009;

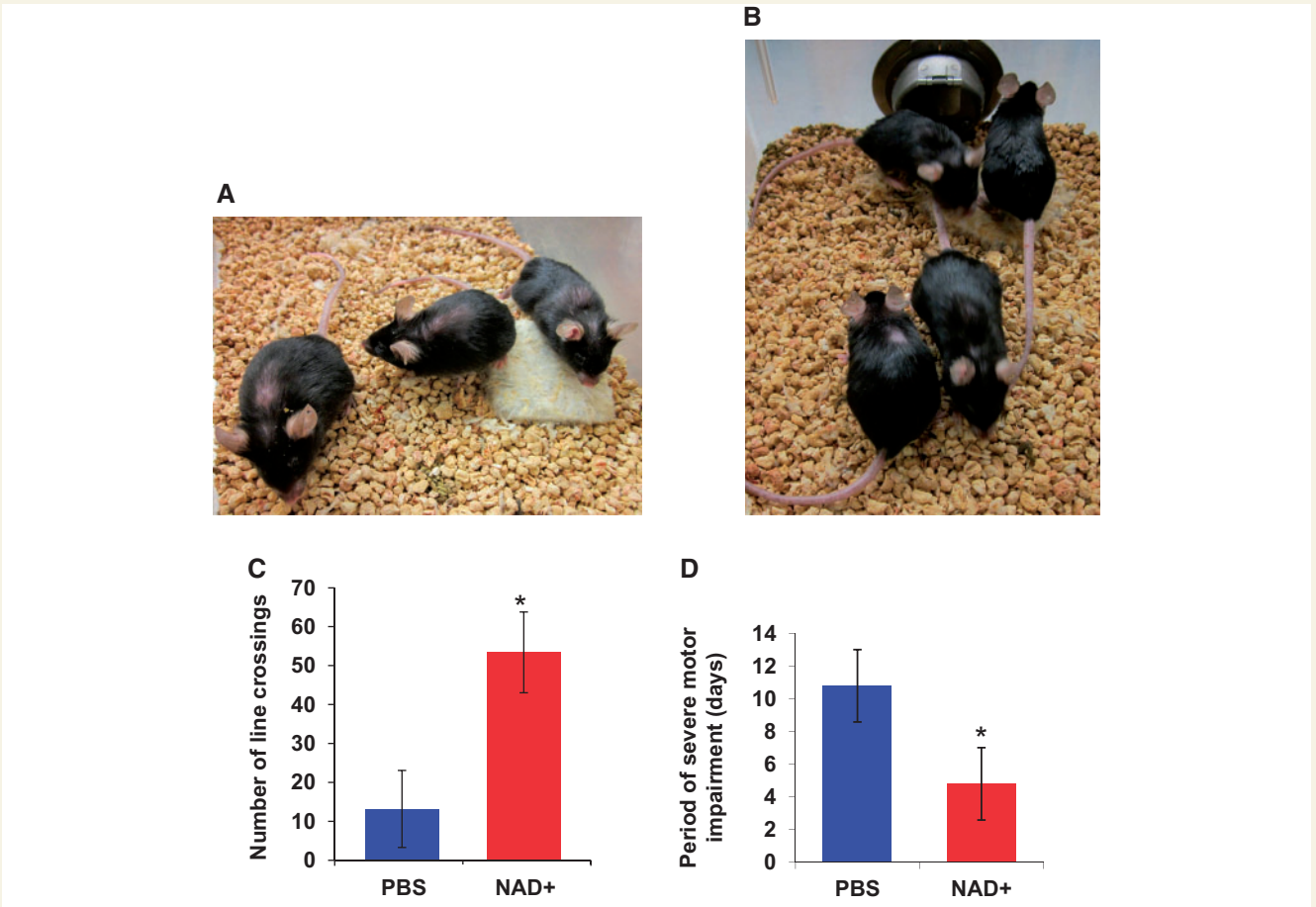


**Figure 7 NAD$^+$ treatment of prion-infected mice during the clinical phase delays disease progression.** (**A** and **B**) NAD$^+$ treatment of prion-infected mice at onset of the clinical phase (Experiment 1). Five mice were treated at 117 days post-intracerebral prion inoculation by daily intranasal NAD$^+$ administration. Five control mice received PBS alone. At the start of the treatment, one mouse of each group was at a more advanced stage of disease and was euthanized shortly thereafter; the other mice exhibited mild signs of motor impairment and were at a similar stage in both groups. Pictures show all remaining mice from the PBS group (**A**) and the NAD$^+$ group (**B**) after 25 days of treatment. (**A**) Mice were not moving; note the ruffled fur, pronounced kyphosis, abnormal position of the ears of all three remaining mice and the abnormal position of the leg of the mouse on the right. This mouse had to be euthanized 2 days after the picture was taken. (**B**) All mice were running, had a conserved fur and mild or no kyphosis. (**C** and **D**) NAD$^+$ treatment of prion-infected mice during the clinical phase (Experiment 2). Five mice were treated at 130 days post-intracerebral prion inoculation by daily intranasal NAD$^+$ administration. Five control mice received PBS alone. (**C**) NAD+-treated mice exhibited enhanced activity in the open field (tested at 134 days post-inoculation, $P = 0.023$). Values are means ± SD. (**D**) The time period during which mice suffered severe motor impairment (starting when mice stayed less than 30 s on the rotarod) was significantly shorter in the NAD$^+$ treated group than in the control group ($P = 0.035$). Values are means ± SD. *Statistically significant difference.

Nixon and Yang, 2012). Overall, the concept has emerged that changes in the quality of the autophagic process are involved in neuronal dysfunction, and that restoring efficient autophagy may be of therapeutic benefit in protein misfolding neurodegenerative diseases by allowing degradation of misfolded protein aggregates (Martinez-Vicente and Cuervo, 2007; Heiseke *et al.*, 2009; Harris and Rubinsztein, 2012). However, the causes of neuronal death in protein misfolding neurodegenerative diseases are still poorly understood, which hampers the development of neuroprotective strategies. To gain understanding of the mechanisms of neurodegeneration linked to misfolding of a host protein, we used the TPrP toxicity model, which is neuron-specific, reproducible, dosable and portable *in vitro* and *in vivo* (Zhou *et al.*, 2012).

Apoptosis and autophagy are salient features of TPrP exposed neurons (Zhou *et al.*, 2012). We started by examining their possible implication in TPrP-induced neuronal death. Our data ruled out apoptosis as a primary cause of cell death, consistent with our earlier observations that apoptosis is a late event in TPrP-induced cell death, occurring after 3 to 4 days of TPrP exposure i.e. after abnormal autophagic activation and extensive vacuolation. Using pharmacological tools, we manipulated various steps of the autophagic pathway. We activated autophagy, blocked autophagy at the early stage of autophagosome formation

or at the step of autophagosome to lysosomal docking, induced lysosome biogenesis or disrupted lysosomal function. None of these treatments significantly altered the time course or amplitude of TPrP-induced neuronal death (Supplementary Fig. 1). These data highlighted that both apoptosis and autophagy are bystanders or downstream contributors, rather than the upstream trigger of the neurodegenerative mechanism.

In sharp contrast, nicotinamide proved to be a critical factor for the rescue of neurons subjected to TPrP injury. Even when added 3 days after TPrP-exposure, nicotinamide, within 3 h, reversed the fate of neuroblastoma cells destined for degeneration, as inferred by the loss of neuritic extensions, cellular vacuolization and, at 3 days, caspase 8 and 9 activation (Fig. 1) (Zhou *et al.*, 2012). This complete rescue indicated that nicotinamide is a key metabolite of the failing pathway in TPrP-treated cells. We determined that the rescuing effect of nicotinamide is because of its role as a precursor of the vital metabolite $NAD^+$, of which TPrP-injured cells are up to 200-fold depleted (Fig. 4). We use the term $NAD^+$ to designate both the oxidized ($NAD^+$) and the reduced (NADH) forms, as TPrP induces starvation of the metabolite and not an imbalance in its redox state. $NAD^+$ is involved in all stages of aerobic respiration leading to ATP production. Thus progressive ATP decrease was observed ~36 h after the onset of $NAD^+$ decrease in TPrP-exposed cells showing that cells suffered from a reduced energy level as a consequence of $NAD^+$ depletion. Interestingly, in accordance with our previous findings that TPrP exerts neuron-specific toxicity (Zhou *et al.*, 2012), primary astrocytes did not suffer from $NAD^+$ depletion after TPrP treatment, but instead exhibited increased $NAD^+$ levels (Supplementary Fig. 6). The significance of this astroglial reaction remains to be investigated, but it might explain why we did not observe a decrease in $NAD^+$ levels in brain homogenates from scrapie-infected mice (not shown).

Addition of exogenous $NAD^+$, which enters cells via the p2X7 ionotropic receptor (Alano *et al.*, 2010; Nikiforov *et al.*, 2011; Pittelli *et al.*, 2011), completely restored viability of TPrP-exposed neuroblastoma cells and primary cortical neurons (Figs 2 and 3).

Cells tightly control their $NAD^+$ levels such that in the liver, $NAD^+$ contents vary depending on the circadian rhythm (Nakahata *et al.*, 2009; Ramsey *et al.*, 2009). $NAD^+$ is a critical co-factor in cytoplasmic glycolysis and mitochondrial aerobic respiration (McCormack and Denton, 1987; Kletzien *et al.*, 1994; Marzulli *et al.*, 1999). $NAD^+$ depletion renders glucose unusable and reduces ATP production. $NAD^+$ depletion also deprives cells of redox capacity via the $NAD^+$/NADH and the $NADP^+$/NADPH cycles. Furthermore, $NAD^+$ is a precursor of second messengers (NAADP and cADPR) indispensable for calcium homeostasis, a function especially critical in neurons (Houtkooper *et al.*, 2010). Finally, $NAD^+$ plays another critical role by catalysing protein deacetylations by sirtuins and the post-translational modifications ADP-ribosylations. Poly-ADP-ribosylation controls DNA repair, gene expression and inflammation (Hassa and Hottiger, 2008), and evidence is emerging that mono-ADP-ribosylation is involved in immune signalling, transcriptional regulation and cell proliferation/death (Welsby *et al.*, 2012). Thus, besides energy deprivation, $NAD^+$ starvation exerts profound and pleiotropic effects on cellular metabolism (summarized in Fig. 8).

How does TPrP induce $NAD^+$ depletion? The fact that $NAD^+$ repletion prevents TPrP toxicity demonstrates that TPrP toxicity is mediated directly by its effect on $NAD^+$ synthesis or catabolism. Using pharmacological and biochemical approaches, we determined that TPrP triggers excessive ADP-ribosylation of cellular proteins (Fig. 5). ADP-ribosylations are known to constitute major $NAD^+$-consuming cellular reactions (Houtkooper *et al.*, 2010). ADP-ribosylation is a dynamic process where addition of ADP-ribose initiates cycles of removal and re-addition of ADP-ribose moieties by specific enzymes (Feijs *et al.*, 2013). This phenomenon is described for both poly- and mono-ADP-ribosylations. Thus an increase of steady-state level of an ADP-ribosylated protein leads to a disproportionately important $NAD^+$ overuse by the cell. Our results therefore suggest that TPrP induces $NAD^+$ depletion downstream of $NAD^+$ synthesis by $NAD^+$ over-consumption, even if at the present time we cannot rule out an additional effect of TPrP elsewhere on $NAD^+$ metabolism.

PARP1 is by far the most widely studied ADP-ribosylation enzyme, and $NAD^+$ depletion has been shown to occur after PARP1 activation (Kauppinen and Swanson, 2007). However, the amounts of poly-ADP-ribosylated (PARylated) proteins were not increased after TPrP exposure, as is the case when PARP1 is activated. Instead, PARylated proteins were reduced starting after 12 h of TPrP exposure in accordance with $NAD^+$ depletion kinetics (Fig. 5E and Fig. 4C). This finding confirmed the results of our pharmacological rescue experiments showing that $NAD^+$ depletion is not due to PARP1 activation. Therefore TPrP induces mono-ADP-ribosylation linked to the activation of a mART that remains to be identified. The existence of oligo-ADP-ribosylations has been postulated [and confirmed in rare instances (Hottiger *et al.*, 2010)] thus at the present time we cannot rule out of their involvement in TPrP-toxicity. Cell membrane associated mARTs are well known; they are also called ecto-ARTs. In contrast, enzymes catalyzing mono-ADP-ribosylation intracellularly have been discovered more recently (Di Girolamo *et al.*, 2013). Although much research is still needed in this field, different ART enzymes are thought to be active in different cell types (Di Girolamo *et al.*, 2005), which might contribute to the neuronal specificity of TPrP toxicity. In conclusion, our study constitutes the first description of $NAD^+$ starvation induced by PARP1 independent ADP-ribosylation.

We also show that apoptosis and autophagy are downstream contributors in the degenerative process triggered by TPrP. Nicotinamide or $NAD^+$ treatment of TPrP-exposed

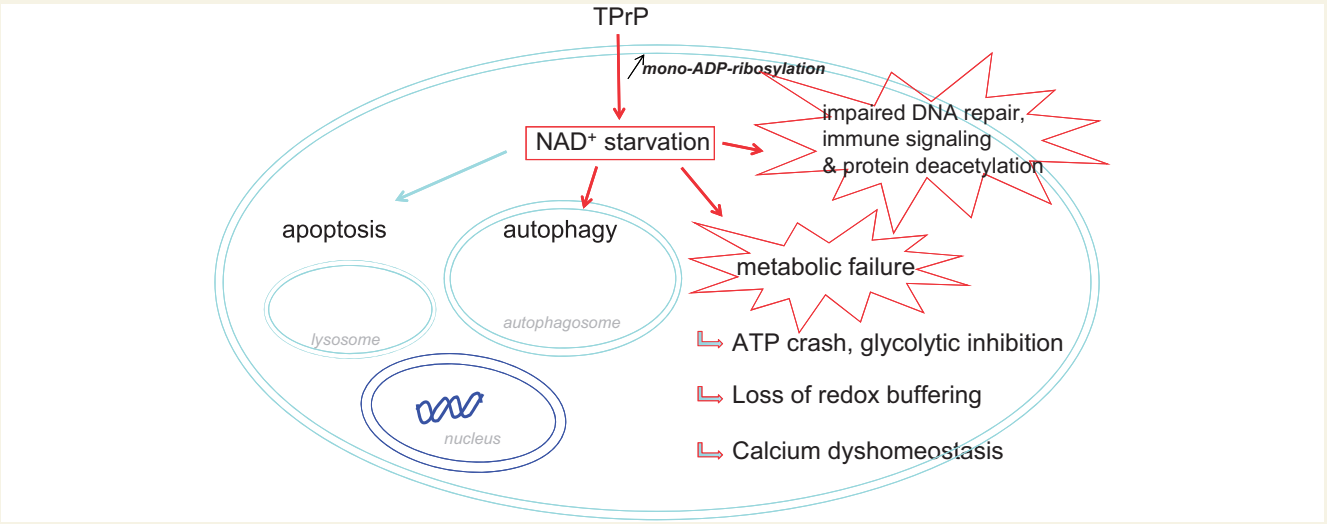


**Figure 8 TPrP-induced neuronal death is due to NAD$^+$ deprivation and multiple metabolic failure.** Our study suggests the following pathogenic mechanism: TPrP enters neuronal cells and induces excessive protein mono-ADP-ribosylation (an NAD$^+$-consuming reaction) resulting in depletion of intracellular NAD$^+$. NAD$^+$ deprivation leads to metabolic failure: (i) NAD$^+$ is necessary for ATP production; NAD$^+$ is also an essential cofactor in glycolysis; glycolytic inhibition induces mitochondrial failure by blocking the flux of glucose-derived pyruvate; (ii) NAD$^+$ is necessary for cellular redox reactions and the ability of cells to survive oxidative stress via the NAD$^+$/NADH and NADP$^+$/NADPH cycles; and (iii) NAD$^+$ is central for intracellular calcium homeostasis because it is the precursor of calcium-regulating molecules NADP$^+$ and cADPR. NAD$^+$ deprivation also leads to impaired DNA repair responses and protein de-acetylation because of its role as a co-factor in ADP-ribosylation and sirtuin-mediated deacetylation reactions. Besides these effects that directly account for cell death, NAD$^+$ starvation activates autophagy (Billington *et al.*, 2008). Caspase 8- and 9-mediated apoptosis (that we described earlier; Zhou *et al.*, 2012) may be induced directly by NAD$^+$ deprivation. However, we cannot exclude that apoptosis be induced by autophagy, as autophagic induction of apoptosis has been described in some instances (Bhoopathi *et al.*, 2010; Lepine *et al.*, 2011).

neurons led to resorption of autophagic vacuoles and prevented apoptosis (Fig. 1). Pharmacological NAD$^+$ deprivation is known to activate the autophagic pathway (Billington *et al.*, 2008). Thus, our data provide a mechanism for autophagy induction by TPrP where TPrP triggers NAD$^+$ depletion which itself results in autophagy activation (Fig. 8). Therefore, our study shows that autophagy triggered by misfolded protein toxicity can be mediated by NAD$^+$ deprivation.

Efficient autophagy relies on lysosomal proteolysis as a last step of the autophagolysosomal pathway. Lysosomes need acidification of their lumen to function properly, a mechanism depending on the activity of the V-type ATPase which uses ATP to pump protons into the lysosomal lumen (Mindell, 2012). The limited ATP supply in TPrP-exposed neurons consequent to NAD$^+$ deprivation is likely to explain the insufficient clearance of autophagic vacuoles in those neurons (Zhou *et al.*, 2012) and maybe also the accumulation of such vacuoles in prion diseases (Liberski *et al.*, 1992). Interestingly, presenilin 1 mutations prevent targeting of the V-ATPase to lysosomes, thereby inducing defective lysosomal function and accumulation of autophagosomes in Alzheimer's disease (Lee *et al.*, 2010), a pathological feature common to prion diseases.

TPrP is highly toxic to pyramidal neurons after stereotaxic injection above the hippocampus (Zhou *et al.*, 2012). Co-injection of NAD$^+$ provided a dose-dependent protection of hippocampal neurons and full protection could be achieved at 100 µM (Fig. 6). We then wanted to verify if these results were relevant for the protection of neurons injured during actual prion infection. Our goal was to determine if it is possible to devise a neuroprotective strategy to provide relief to patients diagnosed with the prion disease Creutzfeldt-Jakob disease. As there is no pre-clinical test for Creutzfeldt-Jakob disease, these patients are diagnosed long after neuroinvasion has occurred, when neurological symptoms are well established (Puoti *et al.*, 2012). To test if NAD$^+$ replenishment could salvage brain function at this late time point we performed two experiments starting daily NAD$^+$ treatments either at the onset of the clinical phase (117 days post-intracerebral prion inoculation) or at 130 days, i.e. well into the clinical phase. In both cases NAD$^+$ treatment improved activity and slowed down the progression of motor impairment. Not surprisingly, given the high prion load of mouse brains at the clinical phase (Lasmézas *et al.*, 1996), NAD$^+$ treatment did not significantly prolong survival times. However, NAD$^+$ treatment significantly increased activity of the mice, improved motor performance and delayed severe motor impairment and paralysis (Fig. 7 and Supplementary Video 1). This effect was remarkable in demonstrating that NAD$^+$ treatment can preserve motor function despite late administration, and suggests that such a treatment might improve the quality of life of patients

with Creutzfeldt-Jakob disease by delaying recumbency. Moreover, combining $NAD^+$ with a drug halting prion replication, when available in the future, might constitute a therapy with neurorestorative potential.

Our study reveals $NAD^+$ depletion as a novel mechanism of neuronal death involved in protein misfolding neurodegenerative diseases. Cell death by excessive activation of PARP1 has been described after excitotoxicity, ischaemia, and oxidative stress and the question is still debated as to whether $NAD^+$ depletion or the products of PARP1, i.e. PARs, cause cell death in these conditions (Andrabi *et al.*, 2011; Siegel and McCullough, 2011). Here, we show that $NAD^+$ depletion itself is the culprit. Much effort has been made to develop PARP1 inhibitors as a neuroprotective strategy but also for the treatment of cancer (Jagtap and Szabo, 2005; Koh *et al.*, 2005). However we found that in the case of TPrP toxicity, $NAD^+$ depletion is not related to PARP1 but to excessive mono-ADP-ribosylation. These results reveal the limits of neuroprotective strategies focusing on PARP1. $NAD^+$ repletion therapy has been shown to protect neurons in rodent models of brain ischaemia/reperfusion injury, Wallerian degeneration of nerves and multiple sclerosis (Kaneko *et al.*, 2006; Sasaki *et al.*, 2006; Ying *et al.*, 2007). Interestingly, $NAD^+$ treatment improved cognitive functions in Alzheimer's disease patients in a randomized, placebo-controlled, double-blinded clinical study (Demarin *et al.*, 2004) and beneficial effects have also been reported in patients with Parkinson's disease (Birkmayer *et al.*, 1990; Kuhn *et al.*, 1996). However, the mechanism of $NAD^+$ protection in these patients has remained highly elusive.

Herein, we demonstrate for the first time that a misfolded amyloidogenic protein can induce neuronal death by genuine $NAD^+$ starvation and that ailing neurons can be completely rescued by $NAD^+$ treatment *in vitro* and by stereotaxic injection *in vivo*, despite the continued presence of the misfolded protein. Importantly, our study shows that neuronal death induced by $NAD^+$ depletion is reversible and that $NAD^+$ replenishment mitigates neurodegeneration in a murine model of advanced prion disease. Our study also questions the role of $NAD^+$ deficiency in other protein misfolding diseases. Meanwhile, we propose the development of $NAD^+$-replenishment strategies for the treatment of prion diseases.

## Acknowledgements

We are grateful to C. Weissmann for support and insightful discussions during this project. We thank Raven Hardy and Gautam Satishchandran for their help.

## Funding

This work was supported by the Scripps Research Institute and by NIH grant RNS081519 (C.L.).

## Supplementary material

Supplementary material is available at *Brain* online.

## References

Aguzzi A, Rajendran L. The transcellular spread of cytosolic amyloids, prions, and prionoids. Neuron 2009; 64: 783–90.

Alano CC, Garnier P, Ying W, Higashi Y, Kauppinen TM, Swanson RA. NAD+ depletion is necessary and sufficient for poly(ADP-ribose) polymerase-1-mediated neuronal death. J Neurosci 2010; 30: 2967–78.

Andrabi SA, Kang HC, Haince JF, Lee YI, Zhang J, Chi Z, et al. Iduna protects the brain from glutamate excitotoxicity and stroke by interfering with poly(ADP-ribose) polymer-induced cell death. Nat Med 2011; 17: 692–9.

Benilova I, Karran E, De Strooper B. The toxic Abeta oligomer and Alzheimer's disease: an emperor in need of clothes. Nat Neurosci 2012; 15: 349–57.

Bhoopathi P, Chetty C, Gujrati M, Dinh DH, Rao JS, Lakka S. Cathepsin B facilitates autophagy-mediated apoptosis in SPARC overexpressed primitive neuroectodermal tumor cells. Cell Death Different 2010; 17: 1529–39.

Biasini E, Unterberger U, Solomon IH, Massignan T, Senatore A, Bian H, et al. A mutant prion protein sensitizes neurons to glutamate-induced excitotoxicity. J Neurosci 2013; 33: 2408–18.

Billington RA, Genazzani AA, Travelli C, Condorelli F. NAD depletion by FK866 induces autophagy. Autophagy 2008; 4: 385–7.

Birkmayer W, Birkmayer JG, Vrecko K, Paletta B. The clinical benefit of NADH as stimulator of endogenous L-dopa biosynthesis in parkinsonian patients. Adv Neurol 1990; 53: 545–9.

Blesa J, Phani S, Jackson-Lewis V, Przedborski S. Classic and new animal models of Parkinson's disease. J Biomed Biotechnol 2012; 2012: 845618.

Braidy N, Gai WP, Xu YH, Sachdev P, Guillemin GJ, Jiang XM, et al. Uptake and mitochondrial dysfunction of alpha-synuclein in human astrocytes, cortical neurons and fibroblasts. Transl Neurodegener 2013; 2: 20.

Büeler H, Raeber A, Sailer A, Fischer M, Aguzzi A, Weissmann C. High prion and PrPsc levels but delayed onset of disease in scrapie-inoculated mice heterozygous for a disrupted PrP gene. Mol Med 1994; 1: 19–30.

Caughey B, Lansbury PT. Protofibrils, pores, fibrils, and neurodegeneration: separating the responsible protein aggregates from the innocent bystanders. Ann Rev Neurosci 2003; 26: 267–98.

Cavallucci V, D'Amelio M, Cecconi F. Abeta toxicity in Alzheimer's disease. Mol Neurobiol 2012; 45: 366–78.

Crystal H, Dickson D, Fuld P, Masur D, Scott R, Mehler M, et al. Clinico-pathologic studies in dementia: nondemented subjects with pathologically confirmed Alzheimer's disease. Neurology 1988; 38: 1682–7.

Demarin V, Podobnik SS, Storga-Tomic D, Kay G. Treatment of Alzheimer's disease with stabilized oral nicotinamide adenine dinucleotide: a randomized, double-blind study. Drugs Exp Clin Res 2004; 30: 27–33.

Di Girolamo M, Dani N, Stilla A, Corda D. Physiological relevance of the endogenous mono(ADP-ribosyl)ation of cellular proteins. FEBS J 2005; 272: 4565–75.

Di Girolamo M, Fabrizio G, Scarpa ES, Di Paola S. NAD(+)-dependent enzymes at the endoplasmic reticulum. Curr TopMed Chem 2013; 13: 3001–10.

Dorandeu A, Wingertsmann L, Chretien F, Delisle MB, Vital C, Parchi P, et al. Neuronal apoptosis in fatal familial insomnia. Brain Pathol 1998; 8: 531–7.

Eliasson MJ, Sampei K, Mandir AS, Hurn PD, Traystman RJ, Bao J, et al. Poly(ADP-ribose) polymerase gene disruption renders mice resistant to cerebral ischemia. Nat Med 1997; 3: 1089–95.

Exner N, Lutz AK, Haass C, Winklhofer KF. Mitochondrial dysfunction in Parkinson's disease: molecular mechanisms and pathophysiological consequences. EMBO J 2012; 31: 3038–62.

Feijs KL, Forst AH, Verheugd P, Luscher B. Macrodomain-containing proteins: regulating new intracellular functions of mono(ADP-ribosyl)ation. Nature reviews. Mol Cell Biol 2013; 14: 443–51.

Friedman-Levi Y, Meiner Z, Canello T, Frid K, Kovacs GG, Budka H, et al. Fatal prion disease in a mouse model of genetic E200K Creutzfeldt-Jakob disease. PLoS Pathog 2011; 7: e1002350.

Garden GA, La Spada AR. Intercellular (mis)communication in neurodegenerative disease. Neuron 2012; 73: 886–901.

Graff CL, Pollack GM. Nasal drug administration: potential for targeted central nervous system delivery. J Pharm Sci 2005; 94: 1187–95.

Haass C, Selkoe DJ. Soluble protein oligomers in neurodegeneration: lessons from the Alzheimer's amyloid beta-peptide. Nat Rev Mol Cell Biol 2007; 8: 101–12.

Harris H, Rubinsztein DC. Control of autophagy as a therapy for neurodegenerative disease. Nat Rev Neurol 2012; 8: 108–17.

Hassa PO, Hottiger MO. The diverse biological roles of mammalian PARPS, a small but powerful family of poly-ADP-ribose polymerases. Front Biosci 2008; 13: 3046–82.

Heiseke A, Aguib Y, Schatzl HM. Autophagy, prion infection and their mutual interactions. Curr Issues Mol Biol 2009; 12: 87–98.

Hottiger MO, Hassa PO, Luscher B, Schuler H, Koch-Nolte F. Toward a unified nomenclature for mammalian ADP-ribosyltransferases. Trends Biochem Sci 2010; 35: 208–19.

Houtkooper RH, Canto C, Wanders RJ, Auwerx J. The secret life of NAD+: an old metabolite controlling new metabolic signaling pathways. Endocrine Rev 2010; 31: 194–223.

Jagtap P, Szabo C. Poly(ADP-ribose) polymerase and the therapeutic effects of its inhibitors. Nat Rev Drug Discov 2005; 4: 421–40.

Kaneko S, Wang J, Kaneko M, Yiu G, Hurrell JM, Chitnis T, et al. Protecting axonal degeneration by increasing nicotinamide adenine dinucleotide levels in experimental autoimmune encephalomyelitis models. J Neurosci 2006; 26: 9794–804.

Kauppinen TM, Swanson RA. The role of poly(ADP-ribose) polymerase-1 in CNS disease. Neuroscience 2007; 145: 1267–72.

Kayed R, Head E, Thompson JL, McIntire TM, Milton SC, Cotman CW, et al. Common structure of soluble amyloid oligomers implies common mechanism of pathogenesis. Science 2003; 300: 486–9.

Kletzien RF, Harris PK, Foellmi LA. Glucose-6-phosphate dehydrogenase: a "housekeeping" enzyme subject to tissue-specific regulation by hormones, nutrients, and oxidant stress. FASEB J 1994; 8: 174–81.

Koh DW, Dawson TM, Dawson VL. Mediation of cell death by poly(ADP-ribose) polymerase-1. Pharmacol Res 2005; 52: 5–4.

Kristiansen M, Deriziotis P, Dimcheff DE, Jackson GS, Ovaa H, Naumann H, et al. Disease-associated prion protein oligomers inhibit the 26S proteasome. Mol Cell 2007; 26: 175–88.

Kuhn W, Muller T, Winkel R, Danielczik S, Gerstner A, Hacker R, et al. Parenteral application of NADH in Parkinson's disease: clinical improvement partially due to stimulation of endogenous levodopa biosynthesis. J Neural Transm 1996; 103: 1187–93.

Kuzhandaivel A, Nistri A, Mladinic M. Kainate-mediated excitotoxicity induces neuronal death in the rat spinal cord *in vitro* via a PARP-1 dependent cell death pathway (Parthanatos). Cell Mol Neurobiol 2010; 30: 1001–12.

Lasmézas CI, Deslys J-P, Demaimay R, Adjou KT, Hauw J-J, Dormont D. Strain specific and common pathogenic events in murine models of scrapie and bovine spongiform encephalopathy. J Gen Virol 1996; 77: 1601–9.

Lasmézas CI, Deslys J-P, Robain O, Jaegly A, Beringue V, Peyrin J-M, et al. Transmission of the BSE agent to mice in the absence of detectable abnormal prion protein. Science 1997; 275: 402–5.

Lee JH, Yu WH, Kumar A, Lee S, Mohan PS, Peterhoff CM, et al. Lysosomal proteolysis and autophagy require presenilin 1 and are disrupted by Alzheimer-related PS1 mutations. Cell 2010; 141: 1146–58.

Lepine S, Allegood JC, Edmonds Y, Milstien S, Spiegel S. Autophagy induced by deficiency of sphingosine-1-phosphate phosphohydrolase 1 is switched to apoptosis by calpain-mediated autophagy-related gene 5 (Atg5) cleavage. J Biol Chem 2011; 286: 44380–90.

Lesne S, Koh MT, Kotilinek L, Kayed R, Glabe CG, Yang A, et al. A specific amyloid-beta protein assembly in the brain impairs memory. Nature 2006; 440: 352–7.

Liberski PP, Brown P. Astrocytes in transmissible spongiform encephalopathies (prion diseases). Folia Neuropathol 2004; ; 42 (Suppl B): 71–88.

Liberski PP, Yanagihara R, Gibbs CJ, Gajdusek DC. Neuronal autophagic vacuoles in experimental scrapie and creutzfeldt-jakob disease. Acta Neuropathol 1992; 83: 134–9.

Luk KC, Kehm V, Carroll J, Zhang B, O'Brien P, Trojanowski JQ, et al. Pathological alpha-synuclein transmission initiates Parkinson-like neurodegeneration in nontransgenic mice. Science 2012; 338: 949–53.

Ma J, Wollmann R, Lindquist S. Neurotoxicity and neurodegeneration when PrP accumulates in the cytosol. Science 2002; 298: 1781–5.

Martinez-Vicente M, Cuervo AM. Autophagy and neurodegeneration: when the cleaning crew goes on strike. Lancet Neurol 2007; 6: 352–61.

Martinez-Vicente M, Talloczy Z, Wong E, Tang G, Koga H, Kaushik S, et al. Cargo recognition failure is responsible for inefficient autophagy in Huntington's disease. Nat Neurosci 2010; 13: 567–76.

Marzulli D, La Piana G, Fransvea E, Lofrumento NE. Modulation of cytochrome c-mediated extramitochondrial NADH oxidation by contact site density. Biochem Biophys Res Commun 1999; 259: 325–30.

McCormack JG, Denton RM. The role of Ca2+ in the regulation of intramitochondrial energy production in heart. Biomed Biochim Acta 1987; 46: S487–92.

Mindell JA. Lysosomal acidification mechanisms. Ann Rev Physiol 2012; 74: 69–86.

Moreno JA, Radford H, Peretti D, Steinert JR, Verity N, Martin MG, et al. Sustained translational repression by eIF2alpha-P mediates prion neurodegeneration. Nature 2012; 485: 507–11.

Nakahata Y, Sahar S, Astarita G, Kaluzova M, Sassone-Corsi P. Circadian control of the NAD+ salvage pathway by CLOCK-SIRT1. Science 2009; 324: 654–57.

Nikiforov A, Dolle C, Niere M, Ziegler M. Pathways and subcellular compartmentation of NAD biosynthesis in human cells: from entry of extracellular precursors to mitochondrial NAD generation. J Biol Chem 2011; 286: 21767–78.

Nixon RA, Wegiel J, Kumar A, Yu WH, Peterhoff C, Cataldo A, et al. Extensive involvement of autophagy in Alzheimer disease: an immuno-electron microscopy study. J Neuropathol Exp Neurol 2005; 64: 113–22.

Nixon RA, Yang DS. Autophagy and neuronal cell death in neurological disorders. Cold Spring Harbor perspectives in biology 2012; 4. pii: a008839.

Olanow CW, Brundin P. Parkinson's disease and alpha synuclein: is Parkinson's disease a prion-like disorder? Mov Disord 2013; 28: 31–40.

Outeiro TF, Putcha P, Tetzlaff JE, Spoelgen R, Koker M, Carvalho F, et al. Formation of toxic oligomeric alpha-synuclein species in living cells. PLoS One 2008; 3: e1867.

Piccardo P, Manson JC, King D, Ghetti B, Barron RM. Accumulation of prion protein in the brain that is not associated with transmissible disease. Proc Natl Acad Sci USA 2007; 104: 4712–17.

Pittelli M, Felici R, Pitozzi V, Giovannelli L, Bigagli E, Cialdai F, et al. Pharmacological effects of exogenous NAD on mitochondrial

bioenergetics, DNA repair, and apoptosis. Mol Pharmacol 2011; 80: 1136–46.

Prusiner SB. Novel proteinaceous infectious particles cause scrapie. Science 1982; 216: 136–44.

Puoti G, Bizzi A, Forloni G, Safar JG, Tagliavini F, Gambetti P. Sporadic human prion diseases: molecular insights and diagnosis. Lancet Neurol 2012; 11: 618–28.

Ramsey KM, Yoshino J, Brace CS, Abrassart D, Kobayashi Y, Marcheva B, et al. Circadian clock feedback cycle through NAMPT-mediated NAD + biosynthesis. Science 2009; 324: 651–4.

Ross TM, Martinez PM, Renner JC, Thorne RG, Hanson LR, Frey WH, 2nd. Intranasal administration of interferon beta bypasses the blood-brain barrier to target the central nervous system and cervical lymph nodes: a non-invasive treatment strategy for multiple sclerosis. J Neuroimmunol 2004; 151: 66–77.

Rumbaugh G, Adams JP, Kim JH, Huganir RL. SynGAP regulates synaptic strength and mitogen-activated protein kinases in cultured neurons. Proc Natl Acad Sci U S A 2006; 103: 4344–51.

Sandberg MK, Al-Doujaily H, Sharps B, Clarke AR, Collinge J. Prion propagation and toxicity *in vivo* occur in two distinct mechanistic phases. Nature 2011; 470: 540–2.

Sasaki Y, Araki T, Milbrandt J. Stimulation of nicotinamide adenine dinucleotide biosynthetic pathways delays axonal degeneration after axotomy. J Neurosci 2006; 26: 8484–91.

Siegel C, McCullough LD. NAD + depletion or PAR polymer formation: which plays the role of executioner in ischaemic cell death? Acta Physiol (Oxf) 2011; 203: 225–34.

Sonati T, Reimann RR, Falsig J, Baral PK, O'Connor T, Hornemann S, et al. The toxicity of antiprion antibodies is mediated by the flexible tail of the prion protein. Nature 2013; 501: 102–6.

Soto C, Satani N. The intricate mechanisms of neurodegeneration in prion diseases. Trends Mol Med 2011; 17: 14–24.

Thellung S, Gatta E, Pellistri F, Corsaro A, Villa V, Vassalli M, et al. Excitotoxicity through NMDA receptors mediates cerebellar granule neuron apoptosis induced by prion protein 90-231 fragment. Neurotox Res 2013; 23: 301–14.

Trancikova A, Ramonet D, Moore DJ. Genetic mouse models of neurodegenerative diseases. Progr Mol Biol Transl Sci 2011; 100: 419–82.

Unterberger U, Voigtlander T, Budka H. Pathogenesis of prion diseases. Acta Neuropathol 2005; 109: 32–48.

Welsby I, Hutin D, Leo O. Complex roles of members of the ADP-ribosyl transferase super family in immune defences: looking beyond PARP1. Biochem Pharmacol 2012; 84: 11–20.

Winner B, Jappelli R, Maji SK, Desplats PA, Boyer L, Aigner S, et al. *In vivo* demonstration that alpha-synuclein oligomers are toxic. Proc Natl Acad Sci USA 2011; 108: 4194–9.

Winslow AR, Rubinsztein DC. The Parkinson disease protein alpha-synuclein inhibits autophagy. Autophagy 2011; 7: 429–31.

Yau L, Elliot T, Lalonde C, Zahradka P. Repression of phosphoenolpyruvate carboxykinase gene activity by insulin is blocked by 3-aminobenzamide but not by PD128763, a selective inhibitor of poly(ADP-ribose) polymerase. Eur J Biochem 1998; 253: 91–100.

Ying W, Wei G, Wang D, Wang Q, Tang X, Shi J, et al. Intranasal administration with NAD + profoundly decreases brain injury in a rat model of transient focal ischemia. Front Biosci 2007; 12: 2728–34.

Zetterberg H, Blennow K. Biomarker evidence for uncoupling of amyloid build-up and toxicity in Alzheimer's disease. Alzheimer's Dement 2013; 9: 459–62.

Zhang J, Dawson VL, Dawson TM, Snyder SH. Nitric oxide activation of poly(ADP-ribose) synthetase in neurotoxicity. Science 1994; 263: 687–89.

Zheng Z, Diamond MI. Huntington disease and the huntingtin protein. Prog Mol Biol Transl Sci 2012; 107: 189–214.

Zhou M, Ottenberg G, Sferrazza GF, Lasmezas CI. Highly neurotoxic monomeric alpha-helical prion protein. Proc Natl Acad Sci USA 2012; 109: 3113–18.